

RSC Advances



This is an *Accepted Manuscript*, which has been through the Royal Society of Chemistry peer review process and has been accepted for publication.

Accepted Manuscripts are published online shortly after acceptance, before technical editing, formatting and proof reading. Using this free service, authors can make their results available to the community, in citable form, before we publish the edited article. This *Accepted Manuscript* will be replaced by the edited, formatted and paginated article as soon as this is available.

You can find more information about *Accepted Manuscripts* in the [Information for Authors](#).

Please note that technical editing may introduce minor changes to the text and/or graphics, which may alter content. The journal's standard [Terms & Conditions](#) and the [Ethical guidelines](#) still apply. In no event shall the Royal Society of Chemistry be held responsible for any errors or omissions in this *Accepted Manuscript* or any consequences arising from the use of any information it contains.

PAPER

A Novel Self-Seeding Polyol Synthesis of Ag Nanowires Using mPEG-b-PVP Diblock Copolymer

Cite this: DOI: 10.1039/x0xx00000x

Hesong Zhao,^{a,||} Jianwei Jiang,^{a,||} Young S. Lim,^b Sangho Kim^{a,*} and Longhai Piao^{a,*}

Received 00th January 2014,
Accepted 00th January 2014

DOI: 10.1039/x0xx00000x

www.rsc.org/rscadvances

The homopolymer of poly(N-vinylpyrrolidone) (PVP) is typically chosen as a capping agent for the polyol synthesis of silver nanowires (Ag NWs). In this paper, we first introduced methoxy poly(ethylene glycol)-b-PVP diblock copolymer (mPEG-b-PVP), which was synthesized by reversible addition-fragmentation transfer (RAFT) polymerization, as a capping agent instead of the PVP homopolymer to the polyol process. Ag NWs were successfully synthesized by this self-seeding process without the additional of any other additives, such as metal salt or exotic seed. The Ag NWs were analyzed by field emission-scanning electron microscopy (FE-SEM), transmission electron microscopy (TEM), X-ray diffraction (XRD) and Fourier transform-infrared spectroscopy (FT-IR). In addition, the relationship between the final morphology of the products and the reaction parameters, such as the molar ratio of mPEG-b-PVP to AgNO₃, injection rate, and temperature, were studied. Finally, under the optimum conditions, the Ag NWs, which were nearly uniform in size, measured 60 to 75 nm in diameter and were as long as ~20 μm. Notably, the synthesized Ag NWs can be dispersed in a non-polar solvent due to the surface PEG tails. This improvement in the dispersion stability may broaden the application of Ag NWs.

1. Introduction

Over the past decade, many methods have been developed for preparing Ag NWs with controllable sizes, including the hydrothermal reaction,^{1,2} ultraviolet irradiation method,^{3,4} electrochemical techniques,^{5,6} DNA/porous material template synthesis,^{7,8} and the polyol process.⁹⁻¹¹ Among these methods, the polyol process has been extensively exploited by numerous research groups due to its low cost, high yield, and simplicity. In this process, AgNO₃ was used as the Ag source, and ethylene glycol (EG) was used as both the solvent and reducing agent. In addition, PVP was employed as a stabilizing agent. Various additives, such as FeCl₃,¹² CuCl₂,¹³ Na₂S,¹⁴ NaCl,¹⁵ PtCl₂,¹⁶ AgCl,¹⁷ KNO₃,¹⁸ AgBr,¹⁹ and HCl,²⁰ have been commonly employed and determined to play an essential role in the selective formation of Ag NWs.

The cations or anions from these additives are crucial for the seed formation and uniaxial growth of multiple twinned particles for the polyol synthesis of Ag NWs.^{12,13} For example, trace amounts of FeCl₃ or CuCl/CuCl₂ have been used to synthesize Ag NWs. The cation (Fe²⁺ or Cu⁺) formed from the reduction of Fe³⁺ or Cu²⁺ by EG can remove the adsorbed oxygen from the surface of twinned seeds, which prevents the dissolution of the seeds and facilitates the growth of Ag NWs. Cl⁻ anions can decrease the concentration of free Ag⁺ in the nucleation stage and selectively etch away many of the nucleation sites in the presence of oxygen, which would promote Ag NWs formation.²¹ In addition, the adsorbed Cl⁻ anions on the surface of Ag nanoparticles could provide

electrostatic stabilization preventing nanoparticle aggregation and inducing Ag NWs growth.¹⁰ Chen and co-workers also reported the fabrication of Ag NWs via a solvothermal method in the presence of AgNO₃, EG, PVP, and trace amounts of Na₂S.¹⁴ The Ag₂S colloids formed in the early stages helped to reduce the concentration of free Ag⁺ ions in the nucleation stage, which subsequently slowly released Ag⁺ ions to the solution and facilitated Ag NW growth. Recently, Schuette and Buhro reported that the early addition of NaCl in the polyol synthesis of Ag NWs results in the rapid formation AgCl nanocubes, which induced the heterogeneous nucleation of Ag on their surfaces, and Ag NWs grow from these nucleation sites.⁹ The crystal structure and lattice constants of Pt are similar to those of Ag.^{16,22} Therefore, a Pt seed, which was produced by the in situ reduction of H₂PtCl₆ or PtCl₂ with EG, is a good nuclei candidate for the epitaxial growth of Ag NWs. Although the salt-assisted process appears to be simple and much progress has been made on elucidating the mechanism of the polyol synthesis of Ag NWs, a clear understanding of the NW formation is still lacking. In addition, these reaction processes are typically difficult to control. Without fine control of reactant concentrations, especially the additives, some by-products, such as nanocubes or nanospheres, can be produced from the growth of isotropic seeds.²³ In addition, it is difficult to synthesize Ag NWs in high purity by the polyol method in the presence of additives.

To obtain Ag NWs with high purity, the self-seeding (without adding exotic metal or salt) method was developed but rarely used. Zhang et al. tried to avoid using exotic additives

and developed a steel-assisted polyol method to produce Ag NWs in high yield.²⁴ They proposed that the chemical etching of multiple twinned particles by in situ formed nitric acid was responsible for the lack of Ag NW formation. The presence of stainless steel could effectively consume the nitric acid and ensure the mass production of Ag NWs. Although this method does not require fine control of the additive amounts, stainless steel was also introduced in the product.²⁵ In 2002, Xia and Sun reported a novel self-seeding process in which AgNO₃ and a PVP solution in EG were simultaneously injected into refluxed EG through a two-channel syringe pump.²⁶ By controlling the injection rate, Ag nanoparticles, which formed in the initial stage of the reduction reaction, could serve as seeds for the subsequent growth of Ag NWs. However, the as-synthesized Ag NWs contained a large amount of nanoparticles when the average molecular weight of PVP was less than 55,000 g/mol. Recently, Mao and co-workers carefully studied Xia's self-seeding method and demonstrated that the selective adsorption of PVP on the side surfaces [100] and end surfaces [111] plays a crucial role in the growth of Ag NWs.²⁷ However, the as-synthesized product contained a large amount of micro-particles and required complex purification. In addition, Zhu et al. proposed another mechanism for the self-seeding method.²⁸ They reported that the yield and aspect ratios of the Ag NWs are substantially influenced by the molecular weight of the PVP surfactant. The product was dominated by NWs when the molecular weight of PVP was 800,000 g/mol. Zhu et al. proposed that the chemical adsorption of Ag⁺ on the PVP chains in the initial stage promoted the growth of the Ag NWs. A Teflon-lined autoclave device was also introduced to synthesize Ag NWs under harsh conditions, such as high pressure and high temperature, without additives or exotic seeds.²⁹ However, the Ag NWs synthesized with this method were the result of end-to-end fusion of two nanorods and exhibited a bending V-shape.

In both the conventional or self-seeding polyol process, the PVP homopolymer was always chosen as the surfactant for the synthesis of Ag NWs. PVP preferentially adsorbs on the [100] facets of the multiple twinned seeds with a decahedral shape, which leads to growth along the <110> direction resulting in Ag NWs. Therefore, the Ag NWs obtained from the polyol process were coated with PVP, which causes only the NWs to disperse in polar solvents, such as water and ethanol. To disperse Ag NWs in a non-polar medium, they have to pass through a ligand-exchange process. Although a number of methods have been reported to transfer Ag or Au nanoparticles/rods from aqueous to organic media,³⁰⁻³³ few of these approaches were suitable for large anisotropic nanoparticles, such as Ag NWs, due to the large van der Waals interactions between the Ag NWs.

In this work, we first introduced mPEG-b-PVP diblock copolymer as a surfactant to the self-seeding polyol synthesis of Ag NWs. The Ag NWs, which had a uniform size with diameters of 60-75 nm and lengths of up to ~20 μm, could be produced in high yield and high purity. In addition, the Ag NWs disperse in polar media, such as water and ethanol, and organic media, such as toluene and THF, due to the PEG block on the surface, which may extend the range of Ag NW applicability.

2. Experimental Section

2.1 Materials and Methods

N-Vinylpyrrolidone (VP) (Aldrich, 99%) was dried over anhydrous magnesium sulfate and purified by distillation under reduced pressure. Tetrahydrofuran (THF) (Aldrich, 99.9%) was purified by distillation from lithium aluminum hydride. Dichloromethane (≥99.9%), poly (ethylene glycol) methyl ether (mPEG-OH) (Mn = 5000 g/mol), 2,2'-Azobis(2-methylpropionitrile) (AIBN) solution (0.2 M in toluene), potassium O-ethylthiocarbonate, 2-bromopropionyl bromide, pyridine, PVP (Mw = 55,000 g/mol and Mw = 29,000 g/mol), AgNO₃, and anhydrous ethylene glycol (EG) were obtained from Sigma-Aldrich and used without further purification. The molecular weights and polydispersity indices of the mPEG-b-PVP diblock copolymer and mPEG were determined by gel permeation chromatography (GPC) using water as the mobile phase at a flow rate of 1.0 mL/min with a PL-GPC 50 detector. The molecular weights were calibrated against PEG standards. Proton nuclear magnetic resonance (¹H NMR) spectra were recorded on a Bruker AV 400 using tetramethylsilane as an internal reference in CDCl₃. The morphology of the Ag nanostructures was observed with a Hitachi S-4800 FE-SEM at an acceleration voltage of 10 kV. The crystal structure of the Ag NWs was characterized by XRD using a diffractometer (DMAX-2000(18 kW)) with Cu Kα radiation (λ=0.154 nm). The evolution of the Ag nanostructures was tracked by ultraviolet-visible (UV-Vis) absorption spectra using a Scinco-S4100 spectrophotometer. FT-IR spectra were measured in a Shimadzu IRAffinity-1 spectrometer using KBr pellets. Microstructural characterizations were performed using TEM (JEM-4010, JEOL) operated at 400 kV.

2.2 Synthesis of macro chain transfer agent mPEG-X.

2.2.1 Synthesis of mPEG-Br.

mPEG-OH (50.0 g), pyridine (2.0 mL), and dichloromethane (100 mL) were added to a flask with a magnetic bar. While the mixture was still cold, 2-bromopropionyl bromide (2.40 mL) was slowly added. The mixture was stirred for 16 h at room temperature, and white precipitates were formed. Dichloromethane (300 mL) was added to the filtrate after the white precipitate was filtered off. The solution was washed with saturated ammonium chloride (4 × 50 mL), saturated sodium hydrogen carbonate (4 × 50 mL), and water (50 mL) and dried over anhydrous magnesium sulfate. Finally, the solvents were evaporated under vacuum.

2.2.2 Synthesis of mPEG-X.

mPEG-Br (5.0 g), pyridine (4.2 mL), and dichloromethane (15 mL) were placed in a flask with a magnetic bar. Potassium O-ethyl xanthate (0.48 g) was added slowly. The mixture was stirred at room temperature for 16 h. Dichloromethane (140 mL) was added to the filtrate after the white precipitate was filtered off. The solution was washed with concentrated ammonium chloride (4 × 40 mL), saturated sodium bicarbonate (4 × 40 mL), and water (50 mL) and dried over anhydrous magnesium sulfate. Then, the crude product was isolated by precipitation in diethylether, and the resulting powder was purified via Soxhlet extraction with diethylether overnight.

2.3 Synthesis of mPEG-b-PVP through RAFT polymerization.

VP (8.0 g), AIBN solution (0.4 mL), mPEG-X (0.8 g), and THF (15 mL) were placed in a Schlenk flask and degassed via freeze-pump-thaw cycles. The flask was immersed in an oil bath preheated at 60 °C. After 15 h, mPEG-b-PVP was isolated by precipitation in diethylether.

2.4 Synthesis of Ag NWs using mPEG-b-PVP.

In a typical synthesis of Ag NWs, EG (5 mL) was heated at 160 °C for 1 hour in a three-neck flask. The EG solutions of mPEG-b-PVP (0.28 g, 3 mL) and AgNO₃ (0.08 g, 3 mL) were simultaneously added to the three-neck flask using a two-channel syringe pump at a rate of 0.1 mL/min. The reaction mixture was heated at 160 °C for 60 min and cooled to room temperature. The product was isolated by centrifugation at 6000 rpm for 20 min and washed three times with ethanol/acetone (2:1 vol/vol) to remove excess polymers.

2.5 Synthesis of Ag NWs using PVP-55,000 and NaCl.

For comparison, Ag NWs that were ~60 nm in diameter and ~10 μm in length were synthesized using the conventional polyol method.⁹ An EG solution (10 mL) composed of PVP-55,000 (500 mg) and NaCl (8 mg) in a round-bottom flask was heated at 170 °C for 40 min. In the meantime, an EG solution of AgNO₃ (102 mg, 5 mL) was prepared, and the solution (1 mL) was added quickly to the PVP solution with a stirring rate of 1,200 rpm. Then, the remaining AgNO₃ solution (4 mL) was added dropwise at a stirring rate of 600 rpm to the PVP solution over the course of 4 minutes using a disposable pipette. Upon completion of the dropwise addition, the solution was maintained at that temperature for 30 min and finally cooled in air to room temperature. The Ag NW was isolated by centrifugation at 6000 rpm for 20 min and washed twice with ethanol/acetone (2:1 vol/vol).

3. Results and discussion

3.1 Synthesis and characterization of mPEG-b-PVP.

mPEG-b-PVP was synthesized according to a previously published method (Scheme 1) developed by Bert Klumperman with some modifications.³⁴

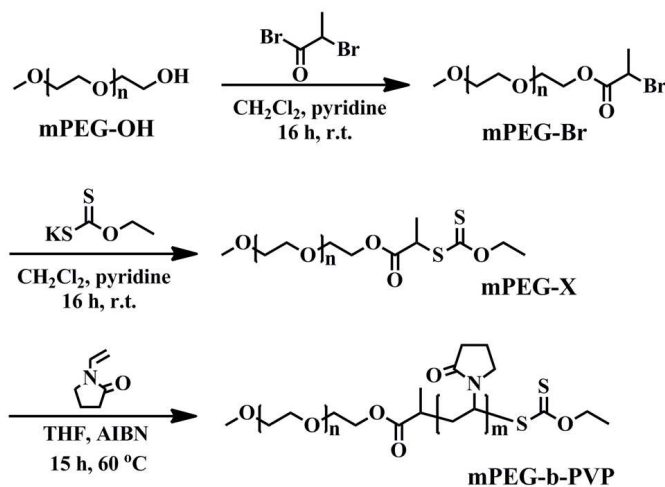


Figure 1 shows the typical GPC curves of mPEG macro-CTA and its chain-extended mPEG-b-PVP. The molecular weights were calibrated against PEG standards. After 15 h of polymerization, the prepolymer peak shifted toward a higher molecular weight ($M_n = 33,800$ g/mol). In addition, these GPC peaks are monomodal and reasonably symmetrical with a

narrow distribution (PDI = 1.03), which indicated the well-controlled behavior of this RAFT polymerization.

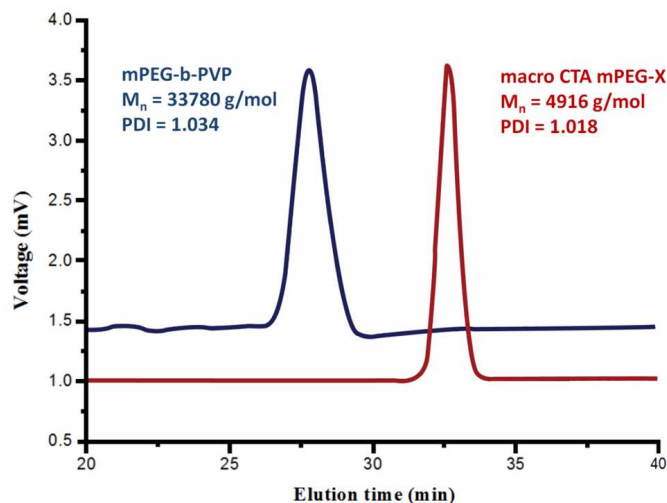


Figure 1. GPC curves of mPEG-X and mPEG-b-PVP.

The structures of mPEG macro-CTA and mPEG-b-PVP were analyzed by ¹H NMR spectroscopy. Peak assignments were made based on the expected structure, which is shown in the inset of Figure 2. The signals at 1.5–2.5 ppm (l, k, r) and 3.0–4.1 ppm (s, j) are due to the repeat units of PVP. The methylene signals of mPEG overlap with the signal for the methine (-CH-) of the repeat unit of PVP. The calculated molecular weight was 38,500 g/mol according to the following equation: $M_n^{\text{NMR}} = 5176 + 114 \times 226 / (A_{s+m} / A_j - 0.5)$ g/mol, where 5176 g/mol and 111 g/mol are the molar mass of mPEG macro-CTA and VP monomer, respectively, and A_{s+m} and A_j are the integration area of the corresponding peaks.

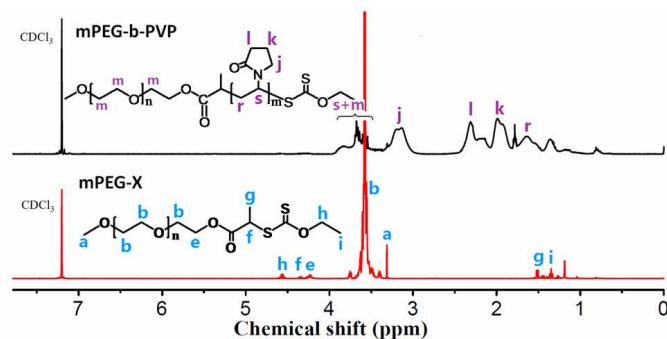


Figure 2. ¹H NMR spectra of macro-CTA and mPEG-b-PVP in CDCl₃ and their respective structures.

3.2 Synthesis and characterization of Ag NWs.

The synthesized mPEG-b-PVP was introduced in the synthesis of Ag NWs, where AgNO₃ and the diblock copolymer solutions in EG were simultaneously injected into the preheated EG using a two-channel syringe pump. Figure 3a shows the SEM image of typical Ag NWs with diameters in the range of 60–75 nm and lengths of up to ~20 μm. The XRD pattern of the Ag NWs (Figure 3b) shows five distinct diffraction peaks at 38.1°, 44.3°, 64.6°, 77.5°, and 81.6° corresponding to the [111], [200], [220], [311], and [222] facets, respectively, of face centered cubic (fcc) Ag crystals (JCPDS 04-0783). The lattice constant calculated from this XRD pattern was 4.082 Å, which was very

close to the literature value of 4.086 Å. No other characteristic peaks were detected in XRD pattern, which indicated the high purity of the fcc Ag crystals produced by the self-seeding polyol process. TEM characterizations of the nanowire were performed to further understand the crystal structure of the products. Figure 3c shows a high-resolution TEM micrograph of the end of an individual Ag NW taken along the <110> zone axis, which indicated that there was a twin plane that divided this NW into two halves. The corresponding selected area electron diffraction (SAED) is shown in Figure 3d. In Figure 3d, extra peaks (denoted by open square) were observed due to the multiplication of the main peaks (denoted by open circle) by the [111] twin plane. This phenomenon is in agreement with previous studies that reported a low threshold for twinning parallel to the [111] faces of fcc metals, such as Ag or Au.^{35,36} Therefore, the TEM and SAED results suggest that the obtained Ag NWs are of a multiple twinned structure.

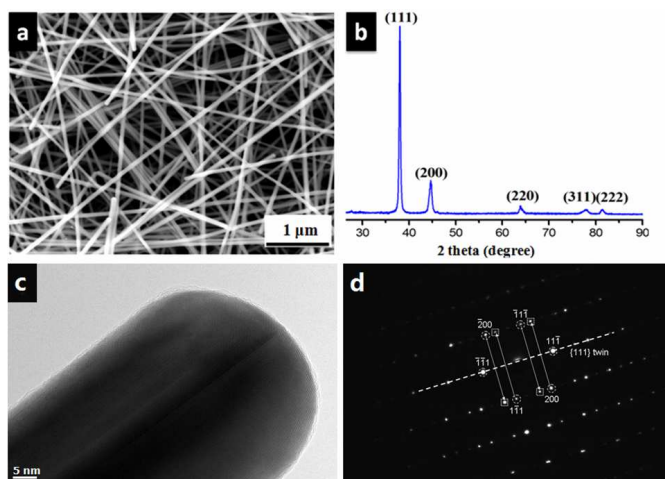


Figure 3. (a) SEM image of Ag NWs, (b) XRD pattern for the Ag NWs, (c) high-resolution TEM image of the end of an individual Ag NW, and (d) the corresponding SAED pattern.

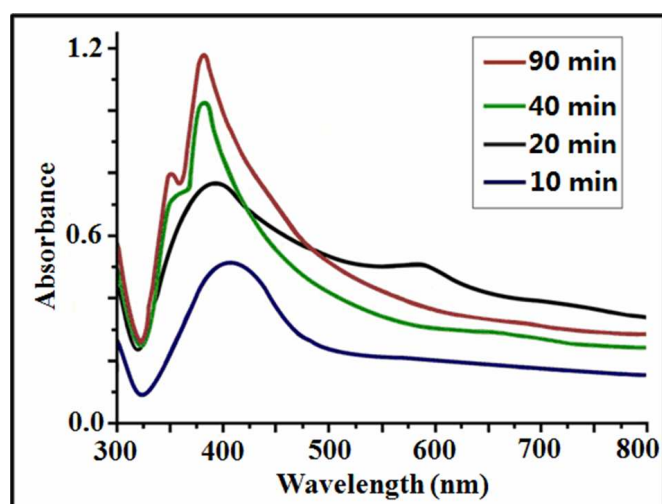


Figure 4. UV-Vis absorption spectra of samples taken from the reaction solution at different nanoparticle growth stages of. All of these solutions were diluted 30 times with water prior to recording the spectra.

Because Ag nanostructures with various shapes and sizes exhibit different surface plasma resonance (SPR), the UV-

visible spectroscopic method was used to track the evolution involved in the process. Figure 4 shows the UV-Vis absorption spectra of the samples recorded at different reaction times after the addition of AgNO₃ and mPEG-b-PVP. The appearance of a broad and intense peak at 405 nm (10 min) indicates the formation of Ag nanoparticles.³⁷ The broad peak indicates the existence of the broad distribution in size and morphology of these Ag nanoparticles. When the reaction proceeded to 20 min, more AgNO₃ was reduced and grown into nanoparticles via Ostwald ripening. In this case, a new peak located at 570 nm was observed, and the previous peak was blue shifted from 405 to 395 nm, which indicated the formation of rod-like structures.³⁸ The peak at 570 nm was due to the longitudinal SPR of the rod-like structures. As the length of the nanorods increased over time (40 min), the intensity of the transverse plasmon mode at 380 nm substantially increased. In addition, the longitudinal plasmon resonance at 570 nm disappeared. A new peak appeared at 350 nm, which was due to the quadruple resonance excitation of the NWs. As the reaction time increased to 90 min, the intensity of the peaks at 350 nm and 380 nm increased, which indicated the formation of a larger aspect ratio for the Ag NWs.¹⁶

Because the reaction was conducted under high temperature (i.e., 160 °C), the weak ester bonds in mPEG-b-PVP (indicated with an arrow in Figure 5a) might be hydrolyzed. To confirm this hypothesis, we compared the FT-IR spectra of mPEG-b-PVP before and after the polyol reaction (Figure 5b). And it was found that the IR spectrum of mPEG-b-PVP diblock copolymer on Ag nanowires differs from that of pure mPEG-b-PVP diblock copolymer. For example, the C=O of PVP after the polyol reaction is blue-shifted from 1661 cm⁻¹ to 1627 cm⁻¹, due to the interaction between PVP and Ag. This result is consistent with the investigations of some other groups.^{25,27,28} In addition, from both curves, the -C-O-C- stretching vibration at 1103 cm⁻¹ from mPEG block were observed.³⁹ Based on these results, it is concluded that the ester bond still existed and the Ag NWs were wrapped with the PVP chain with mPEG tails on the surface.

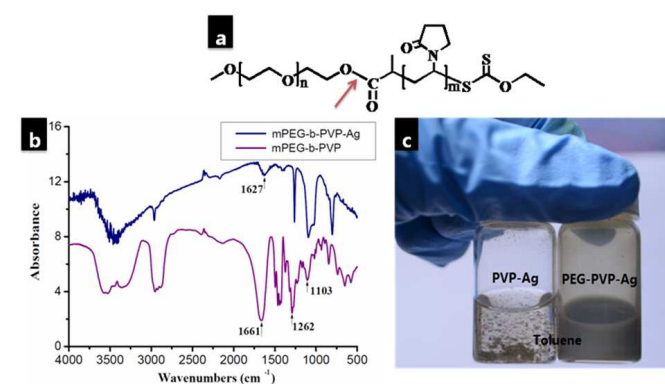


Figure 5. (a) Structure of mPEG-b-PVP and the weak ester bond is indicated with a red arrow, (b) FT-IR spectra of mPEG-b-PVP (purple) and Ag NWs (blue) synthesized with mPEG-b-PVP, and (c) contrast image of the dispersibility in toluene between PVP-Ag NWs and mPEG-b-PVP-Ag NWs (~5 mg/mL).

To understand the role of the mPEG-b-PVP diblock copolymer during the polyol reaction, a controlled experiment with a mixture of mPEG-5000 and PVP-29,000 homopolymer instead of the block copolymer was conducted. Only a large amount of irregular nano- and microparticles were formed

(Fig.S1). Xia and other groups have reported that the synthesized Ag NWs from the self-seeding method with low molecular weight PVP (less than 55,000 g/mol) contained a large amount of micrometer particles due to the low blocking ability of the relatively short PVP chain. Therefore, the formation of Ag NWs in the presence of mPEG-b-PVP cannot be simply explained by the mixed effect of PVP and mPEG homopolymer but may involve short-range synergetic interactions between PVP and mPEG blocks. The detailed mechanism for the formation of the Ag NWs in the presence of mPEG-b-PVP is currently under investigation.

In the conventional polyol synthesis of Ag NWs, various salts, such as NaCl, PtCl₂, FeCl₃, and CuCl₂, were introduced to facilitate the synthesis of Ag NWs. These salts all contain Cl⁻. The introduction of Cl⁻ is widely recognized as being important for the formation of Ag NWs and maintaining the diameter of the Ag NWs below 100 nm. In addition, Cl⁻ combines with oxygen from the air to form Cl⁻/O₂, which can etch and dissolve multiple twinned particles back to a fluctuating structure.¹⁰ Therefore, the Ag NWs always mix with many by-products. In our self-seeding process, there are fewer by-product particles formed due to the self-seeding process that does not require additional salts.

In addition, based on the IR spectrum of the Ag NWs synthesized with mPEG-b-PVP, the surface of the Ag NWs was covered by PVP chains and mPEG tails that face outwards. Therefore, the dispersibility of Ag NWs with mPEG-b-PVP might be much different from that of Ag NWs with the PVP homopolymer. The PVP-Ag NWs and the mPEG-b-PVP-Ag NWs were sonicated for 5 min in toluene. Figure 5c shows that PVP-Ag NWs can barely disperse in toluene forming a flocculent precipitate, and the mPEG-b-PVP-Ag NWs exhibit good dispersibility in toluene. However, the mPEG-b-PVP-Ag NWs precipitated after 1 h and were re-dispersed in toluene again after slight shaking by hand. This result may be due to the low molecular weight of the PEG block and the low viscosity of the solvent.

3.3 Optimization of the reaction conditions for the synthesis of Ag NWs.

To optimize the reaction conditions, the influence of the mPEG-b-PVP/AgNO₃ molar ratio, reaction temperature, and injection rate on the morphology of the Ag nanostructures was investigated.

3.3.1 Molar ratio

The final morphologies of the product are strongly dependent on the molar ratio between mPEG-b-PVP and AgNO₃. Figures 6a-f show the SEM images of the NWs synthesized at different mPEG-b-PVP/AgNO₃ molar ratios. When the molar ratio was lower than 3:1, PVP blocks do not sufficiently cover the [100] facets of multi-twin particles, which results in the growth occurring on both the [111] and [100] faces leading to the formation of NWs with large diameters and masses as well as micrometer-sized particles. By increasing the molar ratio (Figures 6a-d), the diameter of the NWs gradually decreased, and the amount of particles decreased. The optimum mPEG-b-PVP/AgNO₃ molar ratio was determined to be 5:1, as shown in Figure 6d. Under this condition, PVP blocks only passivated the [100] facets of the multi-twin particles, and as the Ag atoms adsorbed on the active [111] facets, the Ag NWs grow along the <110> direction. As the molar ratio increased to 17:1, excess PVP blocks cover both the [100] and [111] facets leading to numerous Ag particles.

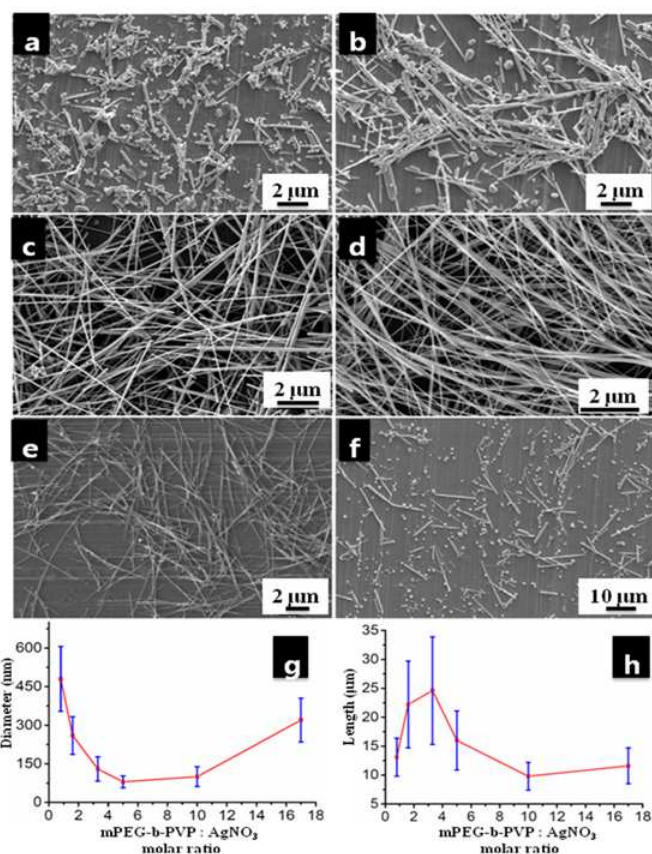


Figure 6. SEM images of Ag NWs synthesized at different mPEG-b-PVP/AgNO₃ molar ratios of (a) 1:1, (b) 2:1, (c) 3:1, (d) 5:1, (e) 10:1, and (f) 17:1. Changes in (g) NW diameter and (h) length with mPEG-b-PVP/AgNO₃ molar ratio are also shown.

3.3.2 Temperature

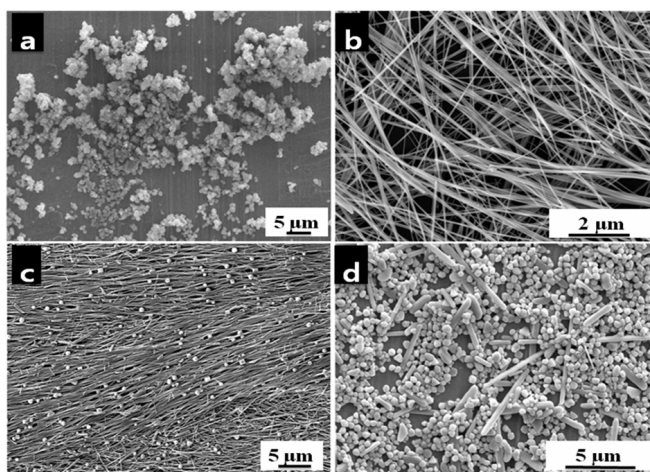


Figure 7. SEM images of Ag NWs synthesized at different temperatures: (a) 150 °C, (b) 160 °C, (c) 170 °C, and (d) 180 °C.

The SEM images of the Ag structures synthesized at 150 °C, 160 °C, 170 °C and 180 °C are shown in Figures 7a-d, respectively. The temperature has a substantial influence on the morphology of Ag structures. When the reaction temperature

was 150 °C, only Ag nanoparticles were formed even after 4 h of reaction. This result was due to glycolaldehyde, which can reduce Ag^+ to Ag atoms and is difficult to transform from EG at this low temperature. At 160 °C, Ag NWs with little particles were synthesized. Under this condition, a suitable thermal energy can produce multi-twin particles at an appropriate rate leading to the growth of Ag NWs with a high yield via Ostwald ripening. Micrometer-sized particles were observed when the reaction temperature increased to 170 °C and were the major product at 180 °C. If the reaction temperature was too high, the excess thermal energy increased the multi-twin particle formation rate, which results in a reaction system that lacks Ag atoms. Therefore, the multi-twin particles tend to dissolve and coalesce with bigger particles via the Ostwald ripening process.

3.3.3 Dropping rate

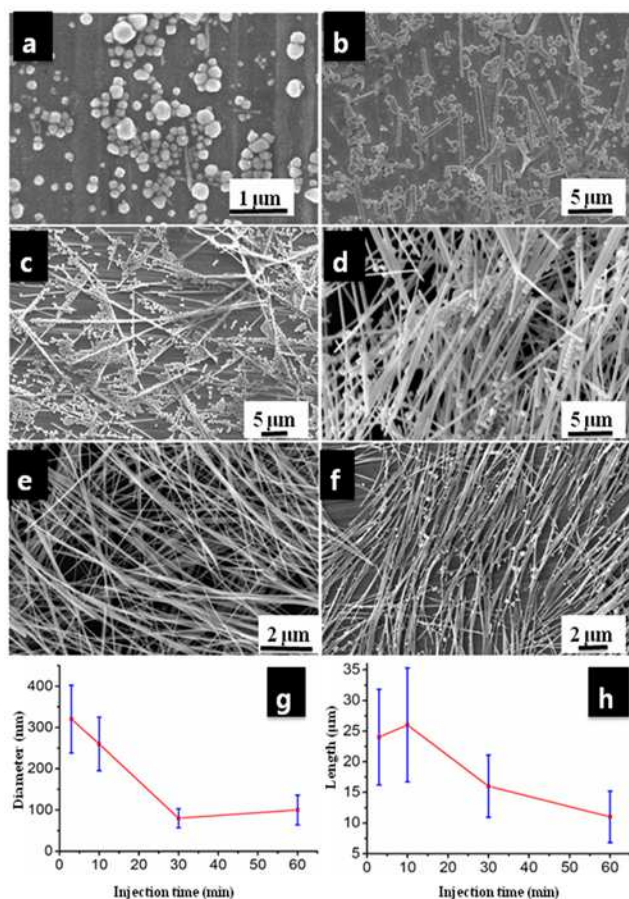


Figure 8. SEM images of Ag NWs synthesized at different dropping rate: (a) 18 mL/min, (b) 3 mL/min, (c) 1 mL/min, (d) 0.3 mL/min, (e) 0.1 mL/min, (f) 0.05 mL/min. Changes in (g) NW diameter and (h) length with injection time are also shown.

Another critical parameter for this self-seeding polyol process is the dropping rate. The SEM images of the Ag structures synthesized with dropping rates of 18 mL/min, 3 mL/min, 1 mL/min, 0.3 mL/min, 0.1 mL/min, and 0.05 mL/min are shown in Figures 8a-f, respectively. At a 18 mL/min dropping rate, large quantities of particles with an irregular morphology were formed. When the dropping rate was decreased, the proportion of one dimensional products increased, and the diameter

decreased (Figures 8a-d). At a 0.1 mL/min dropping rate, Ag NWs with a large aspect ratio and small diameter were obtained. In addition, there were few particles formed in the product (Figure 8e). However, when the dropping rate was continuously decreased, the results tended to be poor. At a dropping rate of 0.05 mL/min, no substantial change in the diameter of the Ag NWs was observed. However, the length decreased, and many particles were formed as by-products. In this case, the clusters and nanoparticles tended to dissolve and coalesce into bigger particles due to the shortage of reduced Ag atoms. Therefore, micrometer-size particles were observed as the product. However, at a high dropping rate (> 0.1 mL/min), a large amount of Ag clusters as formed due to the rapid supersaturation of Ag atoms. These clusters dissolved and coalesced into bigger particles via the Ostwald ripening process rather than forming multi-twin particles. Therefore, the micrometer-sized Ag particles were also formed at a high dropping rate.

4. Conclusions

The mPEG-b-PVP diblock copolymer was successfully introduced in the polyol process for the synthesis of Ag NWs. RAFT polymerization was used to synthesize mPEG-b-PVP with an average molecular weight of 33,800 g/mol and a polydispersity index of 1.03. Ag NWs were synthesized using a self-seeding polyol process with the simultaneous injection of an EG solution containing AgNO_3 and mPEG-b-PVP into the preheated EG solution through a two-channel syringe pump without any exotic additives. The reaction parameters, such as PVP/ AgNO_3 ratio, temperature, and dropping rate, for the synthesis of Ag NWs were studied in detail. Under the optimized conditions, the uniform-sized Ag NWs, which had a diameter of 60-75 nm and length of ~ 20 μm, were produced in high yield and high purity. The Ag NWs with mPEG-b-PVP exhibited superior dispersibility than the one with the PVP homopolymer in a non-polar organic solvent. This improvement in the dispersion stability may broaden the application of Ag NWs. The proposed mechanism for the synthesis of Ag NWs using mPEG-b-PVP is under investigation.

Acknowledgements

This work was supported by the National Research Foundation of Korea (NRF) grant (2012R1A1A4A01009771) funded by the Korea government (MEST).

Notes and references

^a Department of Chemistry, Kongju National University, Chungnam, 314-701, Korea.

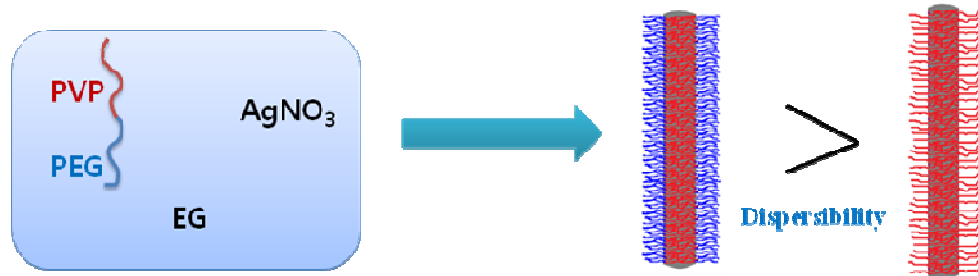
^b Green Ceramics Division, Korea Institute of Ceramic Engineering and Technology, 233-5 Gasan-dong, Geumcheon-gu, Seoul, 153-801, Korea.

[†] These authors contributed equally to the work.

E-mail: sangho1130@kongju.ac.kr, piaohh@kongju.ac.kr.

- Z. Wang, J. Liu, X. Chen, J. Wan and Y. Qian, *Chem. Eur. J.* 2005, **11**, 160-163.
- J. Xu, J. Hu, C. Peng, H. Liu and Y. Hu, *J. Colloid Interface Sci.*, 2006, **298**, 689-693.

- 3 K. Zou, X. H. Zhang, X. F. Duan, X. M. Meng and S. K. Wu, *J. Cryst. Growth*, 2004, **273**, 285-291.
- 4 Y. Zhou, S. H. Yu, C. Y. Wang, X. G. Li, Y. R. Zhu and Z. Y. Chen, *Adv. Mater.*, 1999, **11**, 850-852.
- 5 L. M. Huang, H. T. Wang, Z. B. Wang, A. Mitra, K. N. Bozhilov and Y. S. Yan, *Adv. Mater.*, 2002, **14**, 61-64.
- 6 M. Mazur, *Electrochem. Commun.*, 2004, **6**, 400-403.
- 7 K. Keren, M. Krueger, R. Gilad, G. Ben-Yoseph, U. Sivan and E. Braun, *Science*, 2002, **297**, 72-75.
- 8 S. Berchmans, R. G. Nirmal, G. Prabakaran, S. Madhu and V. Yegnaraman, *J. Colloid Interface Sci.*, 2006, **303**, 604-610.
- 9 S. Coskun, B. Aksoy and H. E. Unalan, *Cryst. Growth Des.*, 2011, **11**, 4963-4969.
- 10 B. Wiley, Y. Sun and Y. Xia, *Acc. Chem. Res.*, 2007, **40**, 1067-1076.
- 11 S. E. Skrabalak, B. J. Wiley, M. Kim, E. V. Formo and Y. Xia, *Nano Lett.*, 2008, **8**, 2077-2081.
- 12 B. Wiley, Y. Sun and Y. Xia, *Langmuir*, 2005, **21**, 8077-8080.
- 13 K. E. Korte, S. E. Skrabalak and Y. Xia, *J. Mater. Chem.*, 2008, **18**, 437-441.
- 14 D. Chen, X. Qiao, X. Qiu, J. Chen and R. Jiang, *J. Colloid Interface Sci.*, 2010, **344**, 286-291.
- 15 W. M. Schuette and W. E. Buhro, *ACS Nano*, 2013, **7**, 3844-3853.
- 16 Y. Sun, B. Gates, B. Mayers and Y. Xia, *Nano Lett.*, 2002, **2**, 165-168.
- 17 L. Hu, H. S. Kim, J.-Y. Lee, P. Peumans and Y. Cui, *ACS Nano*, 2010, **4**, 2955-2963.
- 18 C. L. Kuo and K. C. Hwang, *Langmuir*, 2012, **28**, 3722-3729.
- 19 S. Liu, J. Yue and A. Gedanken, *Adv. Mater.*, 2001, **13**, 656-658.
- 20 S. Chang, K. Chen, Q. Hua, Y. Ma and W. Huang, *J. Phys. Chem. C*, 2011, **115**, 7979-7986.
- 21 L. Gou, M. Chipara and J. M. Zaleski, *Chem. Mater.*, 2007, **19**, 1755-1760.
- 22 M. Tsuji, K. Matsumoto, N. Miyamae, T. Tsuji and X. Zhang, *Cryst. Growth Des.*, 2006, **7**, 311-320.
- 23 K. C. Pradel, K. Sohn and J. Huang, *Angew. Chem. Int. Ed.*, 2011, **50**, 3412-3416.
- 24 W. Zhang, P. Chen, Q. Gao, Y. Zhang and Y. Tang, *Chem. Mater.*, 2008, **20**, 1699-1704.
- 25 Y. Chen, J.-G. Guan and H.-Q. Xie, *Mater. Chem. Phys.*, 2012, **134**, 686-694.
- 26 Y. Sun and Y. Xia, *Adv. Mater.*, 2002, **14**, 833-837.
- 27 H. Mao, J. Feng, X. Ma, C. Wu and X. Zhao, *J. Nanopart. Res.*, 2012, **14**, 1-15.
- 28 J.-J. Zhu, C.-X. Kan, J.-G. Wan, M. Han and G.-H. Wang, *J. Nanomaterials*, 2011, **2011**, 1-7.
- 29 X. C. Jiang, S. X. Xiong, Z. A. Tian, C. Y. Chen, W. M. Chen and A. B. Yu, *J. Phys. Chem. C*, 2011, **115**, 1800-1810.
- 30 G.-T. Wei, Z. Yang, C.-Y. Lee, H.-Y. Yang and C. R. C. Wang, *J. Am. Chem. Soc.*, 2004, **126**, 5036-5037.
- 31 P. J. G. Goulet, G. R. Bourret and R. B. Lennox, *Langmuir*, 2012, **28**, 2909-2913.
- 32 L. Liu and T. L. Kelly, *Langmuir*, 2013, **29**, 7052-7060.
- 33 M. Lista, D. Z. Liu and P. Mulvaney, *Langmuir*, 2014, **30**, 1932-1938.
- 34 G. Pound, F. Aguesse, J. B. McLeary, R. F. M. Lange and B. Klumperman, *Macromolecules*, 2007, **40**, 8861-8871.
- 35 G. Bögel, H. Meekes, P. Bennema and D. Bollen, *J. Phys. Chem. B*, 1999, **103**, 7577-7583.
- 36 S. Link, Z. L. Wang and M. A. El-Sayed, *J. Phys. Chem. B*, 2000, **104**, 7867-7870.
- 37 M. Kerker, *J. Colloid Interface Sci.*, 1985, **105**, 297-314.
- 38 R. M. Dickson and L. A. Lyon, *J. Phys. Chem. B*, 2000, **104**, 6095-6098.
- 39 Y. Sun, M. Chen, Z. Wang and L. Wu, *Chem. Commun.*, 2014, **50**, 5767-5770.



Graphical Table of Contents